JOURNAL OF MAGNETIC RESONANCE 43, 259–281 (1981)

Two-Dimensional Chemical Exchange and Cross-Relaxation Spectroscopy of Coupled Nuclear Spins

S. MACURA,* Y. HUANG,† D. SUTER, AND R. R. ERNST

Laboratorium für Physikalische Chemie, Eidgenössische Technische Hochschule, 8092 Zürich, Switzerland

Received October 30, 1980

The features of two-dimensional cross-relaxation and chemical exchange spectroscopy of coupled spins are investigated theoretically and by experiment. It is shown that spin–spin couplings can lead to *J* cross-peaks in analogy to cross-peaks in two-dimensional autocorrelated spectroscopy. They reflect a coherent magnetization transfer in contrast to the incoherent processes responsible for cross-relaxation and for chemical exchange. Possibilities of selectively suppressing *J* cross-peaks are discussed.

I. INTRODUCTION

Recent experiments have demonstrated that two-dimensional (2D) exchange spectroscopy (*1*) is a powerful and promising technique for the elucidation of chemical exchange processes (*2*) and of magnetization exchange by cross-relaxation, leading to nuclear Overhauser effects (NOE) (*3*, *4*), in a large variety of chemical systems from mixtures of one-spin molecules to complex biological macromolecules. We define here the term "magnetization exchange" or simply "exchange" to comprise both "chemical exchange" and "exchange by cross-relaxation." We combine chemical exchange and cross-relaxation in a unified treatment.

Two-dimensional exchange spectroscopy allows one to trace out complete networks of exchange processes by a surprisingly simple technique resulting in an extraordinarily enlightening 2D map. The appearance of a cross-peak indicates chemical or magnetization exchange between two sites within one molecule or between several molecules. However, this straightforward analysis of 2D exchange spectra is possible only in the absence of spin–spin interactions, for these interactions can also lead to additional cross-peaks in a 2D exchange spectrum. We call them *J* cross-peaks.

J cross-peaks arise from a coherent magnetization transfer via a quantum-mechanical coupling network whereas the chemical exchange and the cross-relaxation or NOE cross-peaks reflect incoherent transfer processes. *J* cross-peaks therefore have characteristic properties different from those of the exchange

* Permanent address: Institute of Physical Chemistry, Faculty of Sciences, 11000 Beograd, Yugoslavia.

† Permanent address: Physics Department, Huadong Normal University, Shangai, P.R. China.

0022-2364/81/050259-23$02.00/0

cross-peaks. There is a close analogy to the cross-peaks well known from 2D autocorrelated spectroscopy (*5–9*). These features enable one to design procedures for their distinction and selective suppression.

The basic scheme of 2D exchange spectroscopy (*1–3*) is sketched in Fig. 1. A first $(\pi/2)_y$ pulse creates transverse magnetization. The following evolution period, t_1, serves to "frequency-label" the various magnetization components by their Larmor frequencies. The time t_1 is varied from experiment to experiment. A second $(\pi/2)_y$ pulse restores the x component along the z axis for the subsequent mixing period of length τ_m during which the slow exchange process may take place. A last $(\pi/2)_y$ pulse again generates transverse magnetization to make evident the product of the exchange process. The major complication in coupled spin systems arises from the additional creation of zero-, single-, double-, and higher-quantum coherence by the second $(\pi/2)_y$ pulse, which is also transformed into observable magnetization by the third pulse. This coherence is responsible for the occurrence of J cross-peaks.

In the next section we present the theoretical basis for 2D chemical exchange and 2D NOE spectroscopy of coupled spin systems. Section III exemplifies the essential features, by an explicit treatment of a weakly coupled two-spin system. Techniques suitable for the suppression of the undesired J cross-peaks are described, finally, in Section IV.

II. THEORY OF MAGNETIZATION EXCHANGE IN COUPLED SPIN SYSTEMS

In this section we give a formal treatment of magnetization exchange in coupled spin systems which is sufficiently general to handle coherent and incoherent exchange processes simultaneously. Readers more interested in the practical aspects of 2D spectroscopy may skip this section and consult the explicit treatment of cross-peaks in a two-spin system described in Section III.

The description of magnetization exchange in systems without spin–spin couplings (*1, 3*) can be based on the Bloch equations modified to include chemical exchange (*10–12*) or cross-relaxation (*13–15*). However, for exchange in coupled nuclear spin systems, it is necessary to use a full density operator treatment.

We start with a generalized density operator equation (*11, 12, 16–19*) which includes both cross-relaxation and chemical exchange processes:

$$\dot{\sigma}(t) = -i[\mathcal{H}, \sigma(t)] - \hat{\hat{\Gamma}}\{\sigma(t) - \sigma_0\} + \hat{\hat{\Xi}}\sigma. \qquad [1]$$

The relaxation superoperator $\hat{\hat{\Gamma}}$ drives the system toward the equilibrium state σ_0 while $\hat{\hat{\Xi}}$ represents the effects of chemical exchange.

The relaxation superoperator $\hat{\hat{\Gamma}}$ is best expressed in terms of the Redfield relaxation matrix (*20, 21*) or in the operator form given by Abragam (*14*). The chemical exchange superoperator $\hat{\hat{\Xi}}$, on the other hand, is conveniently represented in the form (*16*)

$$\hat{\hat{\Xi}}\sigma = \sum_j \frac{1}{\tau_j}[X_j \sigma X_j^{-1} - \sigma]. \qquad [2]$$

The summation here runs over all independent chemical exchange processes of the system considered with the exchange lifetimes τ_j. The operator X_j is the

chemical exchange operator which expresses the reordering of the base functions caused by the chemical exchange process j (*16*). For intermolecular exchange, the situation is somewhat more complicated as it is necessary to enlarge the Hilbert space to include all molecules involved (*16–18*).

The equilibrium density operator σ_0 commutes with the Hamiltonian, $[\mathcal{H}, \sigma_0] = 0$, and is not modified by chemical exchange, $\hat{\Xi}\sigma_0 = 0$. It is therefore possible to write Eq. [1] in the condensed form

$$\frac{d}{dt}(\sigma(t) - \sigma_0) = \hat{L}\{\sigma(t) - \sigma_0\} \qquad [3]$$

with the superoperator $\hat{L}$ representing the combined action of the Hamiltonian superoperator $\hat{\mathcal{H}}$, the relaxation superoperator Γ, and the chemical exchange superoperator $\hat{\Xi}$.

$$\hat{L} = -i\hat{\mathcal{H}} - \hat{\Gamma} + \hat{\Xi}, \qquad \hat{\mathcal{H}}A = [\mathcal{H}, A]. \qquad [4]$$

The evolution of the density operator in a 2D exchange experiment, shown in Fig. 1, can be computed in complete analogy to the procedure developed for 2D correlated spectroscopy (*5*). We denote by $\sigma(0)$ the density operator after preparation by a $\pi/2$ pulse at the beginning of the evolution period. For $\sigma(t_1)$ at the end of the evolution period, we then obtain

$$\sigma(t_1) = \exp(\hat{L}t_1)\sigma(0) + [1 - \exp(\hat{L}t_1)]\sigma_0 \qquad [5]$$

and after the mixing period of length τ_m, we find

$$\sigma(t_1, \tau_m, 0) = \hat{R}_y\left(\frac{\pi}{2}\right)\left\{\exp(\hat{L}\tau_m)\hat{P}\hat{R}_y\left(\frac{\pi}{2}\right)\sigma(t_1) + [1 - \exp(\hat{L}\tau_m)]\sigma_0\right\}. \qquad [6]$$

The superoperator $\hat{R}_y(\pi/2)$ represents here the actions of the $(\pi/2)_y$ pulses at the beginning and at the end of the mixing period,

$$\hat{R}_y\left(\frac{\pi}{2}\right)\sigma = \exp\left(-i\frac{\pi}{2}F_y\right)\sigma\exp\left(i\frac{\pi}{2}F_y\right), \qquad [7]$$

with $F_y = \sum_j I_{jy}$. The projection superoperator $\hat{P}$ expresses the suppression of certain magnetization components during the mixing period by a magnetic field gradient pulse or by phase-shifted pulse sequences (cf. Section IV). During detection, we obtain the density operator

$$\sigma(t_1, \tau_m, t_2) = \exp(\hat{L}t_2)\sigma(t_1, \tau_m, 0) + [1 - \exp(\hat{L}t_2)]\sigma_0. \qquad [8]$$

We are exclusively interested in the cross- and auto-peaks of the resulting 2D spectrum and disregard the axial peaks which originate from terms involving σ_0. We can therefore simplify the expression for $\sigma(t_1, \tau_m, t_2)$ by neglecting all those terms which explicitly depend on σ_0:

$$\sigma(t_1, \tau_m, t_2) = \exp(\hat{L}t_2)\hat{R}_y\left(\frac{\pi}{2}\right)\exp(\hat{L}\tau_m)\hat{P}\hat{R}_y\left(\frac{\pi}{2}\right)\exp(\hat{L}t_1)\sigma(0). \qquad [9]$$

The eigenvalues of the superoperator $\hat{L}$ determine, as usual, resonance frequencies and linewidths of the resonance lines in the 1D spectrum as well as

those of the peaks in the 2D spectrum in both frequency dimensions. The complex peak intensities and phases, on the other hand, are given by the matrix elements

$$I_{kl,mn} = F^{+}_{lk}\left[\hat{\hat{R}}_y\left(\frac{\pi}{2}\right)\exp(\hat{\hat{L}}\tau_m)\hat{\hat{P}}\hat{\hat{R}}_y\left(\frac{\pi}{2}\right)\right]_{kl,mn}\sigma(0)_{mn} \qquad [10]$$

with $F^{+} = \sum_j (I_{jx} - iI_{jy})$.

In general the intensities $I_{kl,mn}$ contain contributions both from random and from coherent exchange processes acting in the course of the mixing time τ_m. The purpose of the experiment, however, is exclusively the pursuit of the random exchange processes coming from chemical exchange or cross-relaxation. The random exchange processes are governed by the relaxation superoperator $\hat{\hat{\Gamma}}$ and the chemical exchange superoperator $\hat{\hat{\Xi}}$. The coherent exchange, on the other hand, is caused by the spin–spin couplings which effect a differential precession of the various coherence components during the mixing period τ_m.

The features of the exchange cross-peaks resulting from Eq. [10] have been discussed extensively elsewhere (*1*, *3*) on the basis of solutions of modified Bloch equations. Here we concentrate on the features of the *J* cross-peaks which occur exclusively in coupled spin systems.

III. CROSS-RELAXATION AND CHEMICAL EXCHANGE IN THE WEAKLY COUPLED TWO-SPIN SYSTEM

The relevant features of 2D exchange spectroscopy in coupled spin systems can most easily be explained by considering a weakly coupled two-spin-1/2 system with the two Larmor frequencies Ω_A and Ω_B and with the scalar spin–spin coupling constant *J*. The system may involve cross-relaxation between nuclei A and B as well as a chemical exchange process interchanging the two nuclei.

(a) Preparation

The experiment starts with the system in thermodynamic equilibrium with the density operator $\sigma_0 = F_z = I_{Az} + I_{Bz}$ (neglecting numerical factors). The first $(\pi/2)_y$ pulse (Fig. 1) creates the initial state $\sigma(0) = F_x = I_{Ax} + I_{Bx}$.

The following evolution for the time t_1 for frequency labeling leads to the density matrix (written in the eigenbase of the Hamiltonian)

$$\sigma(t_1) = \frac{1}{2}\begin{pmatrix} 0 & \beta_2^* & \alpha_2^* & 0 \\ \beta_2 & 0 & 0 & \alpha_1^* \\ \alpha_2 & 0 & 0 & \beta_1^* \\ 0 & \alpha_1 & \beta_1 & 0 \end{pmatrix}, \qquad [11]$$

with the four coherence functions

$$\begin{aligned}
\alpha_1(t_1) &= \exp(i\Omega_{A1}t_1)\cdot\exp(-t_1/T_{2A}), & \Omega_{A1} &= \Omega_A - \omega_1 - J/2,\\
\alpha_2(t_1) &= \exp(i\Omega_{A2}t_1)\cdot\exp(-t_1/T_{2A}), & \Omega_{A2} &= \Omega_A - \omega_1 + J/2,\\
\beta_1(t_1) &= \exp(i\Omega_{B1}t_1)\cdot\exp(-t_1/T_{2B}), & \Omega_{B1} &= \Omega_B - \omega_1 - J/2,\\
\beta_2(t_1) &= \exp(i\Omega_{B2}t_1)\cdot\exp(-t_1/T_{2B}), & \Omega_{B2} &= \Omega_B - \omega_1 + J/2.
\end{aligned} \qquad [12]$$

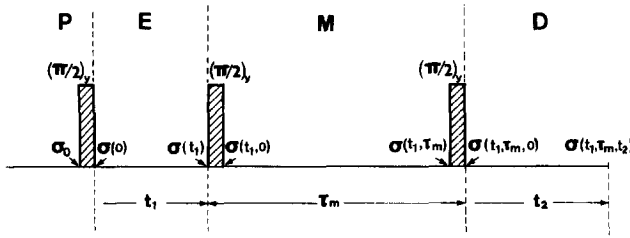

FIG. 1. Basic scheme of 2D exchange spectroscopy with indication of the density operators representing the states of the system. P = preparation period, E = evolution period, M = mixing period, D = detection period.

We designate the four single-quantum transitions of the AB spin system by A_1, A_2, B_1, and B_2 and the corresponding coherence functions by α_1, α_2, β_1, and β_2. The resonance frequencies are indicated in a frame rotating with the carrier frequency ω_1 of the rf pulses. They correspond to the observed frequencies after phase-sensitive detection and are in the audiofrequency range.

The second $(\pi/2)_y$ pulse at the beginning of the mixing period creates the following initial condition for the exchange process:

$$\sigma(t_1, 0) = \frac{1}{4}\begin{pmatrix} -\mathrm{Re}\{\alpha_1 + \alpha_2 + \beta_1 + \beta_2\} & \mathrm{Re}\{\alpha_1 - \alpha_2\} - i\,\mathrm{Im}\{\beta_1 + \beta_2\} \\ \mathrm{Re}\{\alpha_1 - \alpha_2\} + i\,\mathrm{Im}\{\beta_1 + \beta_2\} & \mathrm{Re}\{-\alpha_1 - \alpha_2 + \beta_1 + \beta_2\} \\ i\,\mathrm{Im}\{\alpha_1 + \alpha_2\} + \mathrm{Re}\{\beta_1 - \beta_2\} & i\,\mathrm{Im}\{-\alpha_1 + \alpha_2 + \beta_1 - \beta_2\} \\ i\,\mathrm{Im}\{-\alpha_1 + \alpha_2 - \beta_1 + \beta_2\} & i\,\mathrm{Im}\{\alpha_1 + \alpha_2\} + \mathrm{Re}\{-\beta_1 + \beta_2\} \end{pmatrix}$$

$$\begin{pmatrix} -i\,\mathrm{Im}\{\alpha_1 + \alpha_2\} + \mathrm{Re}\{\beta_1 - \beta_2\} & i\,\mathrm{Im}\{\alpha_1 - \alpha_2 + \beta_1 - \beta_2\} \\ i\,\mathrm{Im}\{\alpha_1 - \alpha_2 - \beta_1 + \beta_2\} & -i\,\mathrm{Im}\{\alpha_1 + \alpha_2\} + \mathrm{Re}\{-\beta_1 + \beta_2\} \\ \mathrm{Re}\{\alpha_1 + \alpha_2 - \beta_1 - \beta_2\} & +\mathrm{Re}\{-\alpha_1 + \alpha_2\} - i\,\mathrm{Im}\{\beta_1 + \beta_2\} \\ \mathrm{Re}\{-\alpha_1 + \alpha_2\} + i\,\mathrm{Im}\{\beta_1 + \beta_2\} & \mathrm{Re}\{\alpha_1 + \alpha_2 + \beta_1 + \beta_2\} \end{pmatrix} . \quad [13]$$

All matrix elements of $\sigma(t_1, 0)$, including the zero- and double-quantum elements, are normally different from zero and affect the following mixing process.

(b) The Mixing Process

The evolution of $\sigma(t_1, \tau_m)$ during the mixing period is of central importance for the study of exchange processes. It is determined by the superoperator $\hat{L}$, defined in Eq. [4], which includes the actions of the Hamiltonian, of relaxation, and possibly of chemical exchange. For the computation of the density operator $\sigma(t_1, \tau_m)$ at the end of the mixing period of length τ_m (Eq. [9]),

$$\sigma(t_1, \tau_m) = \exp\{\hat{L}\tau_m\}\sigma(t_1, 0), \quad [14]$$

it is convenient to consider the elements of $\sigma(t_1, 0)$, Eq. [13], as components of a vector on which the (super)matrix $\exp\{\hat{L}\tau_m\}$ acts. If we order the elements of σ in the following way: diagonal elements (11), (22), (33), (44), zero-quantum coherence (23), (32), single quantum coherence (12), (13), (21), (31), (24), (34), (42), (43), and double-quantum coherence (14), (41), we obtain the supermatrix $(\hat{L})$

$$(\hat{L}) =$$

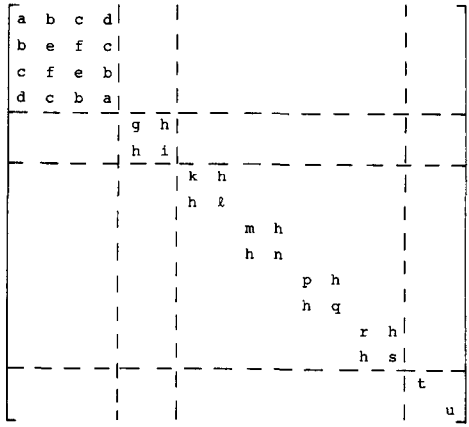

[15]

with the matrix elements

$$\begin{aligned}
a &= -W_{1A} - W_{1B} - W_2 \\
b &= W_{1B} \\
c &= W_{1A} \\
d &= W_2 \\
e &= -W_0 - W_{1A} - W_{1B} - 1/\tau_{AB} \\
f &= W_0 + 1/\tau_{AB} \\
g &= -i(\Omega_A - \Omega_B) - 1/T_2^{(0)} - 1/\tau_{AB} \\
h &= 1/\tau_{AB} \\
i &= i(\Omega_A - \Omega_B) - 1/T_2^{(0)} - 1/\tau_{AB} \\
k &= i(\Omega_B - \omega_1 + J/2) - 1/T_{2B}^{(1)} - 1/\tau_{AB} \\
l &= i(\Omega_A - \omega_1 + J/2) - 1/T_{2A}^{(1)} - 1/\tau_{AB} \\
m &= -i(\Omega_B - \omega_1 + J/2) - 1/T_{2B}^{(1)} - 1/\tau_{AB} \\
n &= -i(\Omega_A - \omega_1 + J/2) - 1/T_{2A}^{(1)} - 1/\tau_{AB} \\
p &= -i(\Omega_A - \omega_1 - J/2) - 1/T_{2A}^{(1)} - 1/\tau_{AB} \\
q &= -i(\Omega_B - \omega_1 - J/2) - 1/T_{2B}^{(1)} - 1/\tau_{AB} \\
r &= i(\Omega_A - \omega_1 - J/2) - 1/T_{2A}^{(1)} - 1/\tau_{AB} \\
s &= i(\Omega_B - \omega_1 - J/2) - 1/T_{2B}^{(1)} - 1/\tau_{AB} \\
t &= -i(\Omega_A + \Omega_B - 2\omega_1) - 1/T_2^{(2)} \\
u &= i(\Omega_A + \Omega_B - 2\omega_1) - 1/T_2^{(2)}
\end{aligned} \qquad [16]$$

Relaxation is represented by the zero-quantum transition probability W_0, the two single-quantum transition probabilities W_{1A} and W_{1B}, and the double-quantum

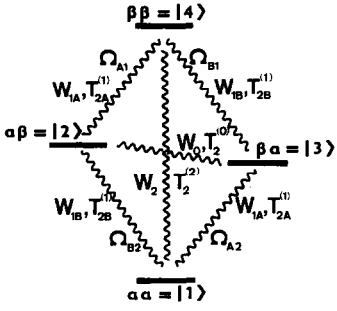

FIG. 2. Transition frequencies Ω, transition probabilities W, and transverse relaxation times T_2 in a weakly coupled two-spin system.

transition probability W_2 and by relaxation rates for zero-quantum coherence, $1/T_2^{(0)}$, for single-quantum coherence of the A and B transitions, $1/T_{2A}^{(1)}$ and $1/T_{2B}^{(1)}$, and for double-quantum coherence, $1/T_2^{(2)}$ (cf. Fig. 2). The average time between two exchange processes is denoted by τ_{AB}.

The matrix $(\hat{L})$ has a characteristic block structure. First, we notice that there are no off-diagonal elements between matrix elements of σ belonging to different orders of transitions. It is therefore natural to separate the density matrix $\sigma(t_1, 0)$ into the four parts

$$\sigma(t_1, 0) = \sigma^{(2)}(t_1, 0) + \sigma^{(0)}(t_1, 0) + \sigma^{(1)}(t_1, 0) + \sigma^{(2)}(t_1, 0). \quad [17]$$

The part $\sigma^{(2)}(t_1, 0)$ consists of the four diagonal elements σ_{11}, σ_{22}, σ_{33}, and σ_{44}, which represent z magnetization, while $\sigma^{(0)}(t_1, 0)$, $\sigma^{(1)}(t_1, 0)$, $\sigma^{(2)}(t_1, 0)$ contain the elements of zero-quantum coherence, σ_{23}, and σ_{32}, single-quantum coherence, σ_{12}, σ_{13}, σ_{21}, σ_{31}, σ_{24}, σ_{34}, σ_{42}, and σ_{43}, and double-quantum coherence, σ_{14} and σ_{41}, respectively. This separation is portrayed in Fig. 3.

The elements representing coherence are connected at most pairwise by the matrix $(\hat{L})$ whereby all off-diagonal elements of $(\hat{L})$ are caused by chemical exchange. In the absence of chemical exchange or for slow exchange, i.e., for $1/\tau_{AB} \ll |\Omega_A - \Omega_B|$, the off-diagonal elements disappear or can be neglected and the transverse coherence components evolve independently.

It turns out that $\sigma^{(2)}(t_1, 0)$ is responsible for cross-relaxation or chemical exchange cross-peaks. The zero-quantum, single-quantum and double-quantum coherences lead to the J cross-peaks. For fast exchange processes $1/\tau_{AB} \sim |\Omega_A - \Omega_B|$, zero- and single-quantum coherence may also affect the exchange cross-peak contribution.

For a detailed discussion of the various contributions to the cross-peaks, we must specify the relevant relaxation mechanisms. We assume (1) relaxation by intramolecular dipolar interaction between A and B nuclei, and (2) external random field relaxation to represent all additional relaxation mechanisms.

(1) Relaxation by Intramolecular Dipolar Interaction

For intramolecular dipolar relaxation, the following expressions apply to Eq. [16],

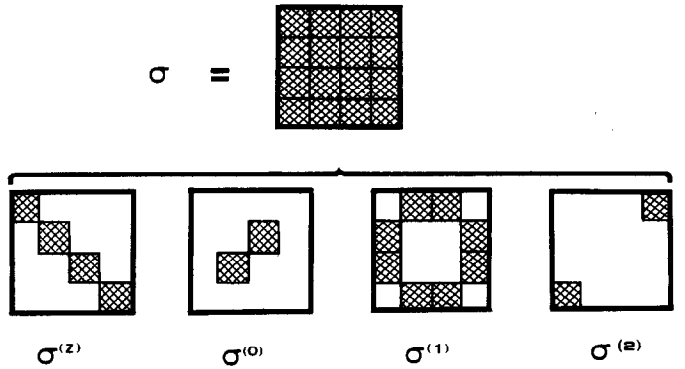

FIG. 3. Subdivision of the density matrix into different orders: $\sigma^{(z)} \rightarrow z$ magnetization, $\sigma^{(0)} \rightarrow$ zero-quantum coherence, $\sigma^{(1)} \rightarrow$ single-quantum coherence, $\sigma^{(2)} \rightarrow$ double-quantum coherence.

$$
\begin{aligned}
1/T_2^{(0)\mathrm{d}} &= (1/4)q_{\mathrm{AB}}[2J(0) + 6J(\Omega)], \\
1/T_{2\mathrm{A}}^{(1)\mathrm{d}} &= 1/T_{2\mathrm{B}}^{(1)\mathrm{d}} = (1/4)q_{\mathrm{AB}}[5J(0) + 6J(\Omega) + 6J(2\Omega)], \\
1/T_2^{(2)\mathrm{d}} &= (1/4)q_{\mathrm{AB}}[6J(\Omega) + 12J(2\Omega)], \\
W_0^{\mathrm{d}} &= (1/2)q_{\mathrm{AB}}J(0), \\
W_{1\mathrm{A}}^{\mathrm{d}} &= W_{1\mathrm{B}}^{\mathrm{d}} = (3/4)q_{\mathrm{AB}}J(\Omega), \\
W_2^{\mathrm{d}} &= 3q_{\mathrm{AB}}J(2\Omega),
\end{aligned}
\qquad [18]
$$

with the relaxation constant

$$
q_{\mathrm{AB}} = (1/10)(\gamma^2\hbar^2 r_{\mathrm{AB}}^{-3})^2 \qquad [19]
$$

and with the spectral density function

$$
J(\omega) = \frac{2\tau_c}{1 + \omega^2\tau_c^2} \qquad [20]
$$

with the correlation time τ_c of the molecular tumbling process. (The definition of $J(\omega)$ in Ref. (*3*) is different by a factor of 2.) The symbol Ω represents the Larmor frequencies Ω_A and Ω_B of the homonuclear spin system.

In the *extreme narrowing limit*, for short correlation time, $\tau_c \ll 1/\Omega$, we find

$$
\begin{aligned}
1/T_2^{(0)\mathrm{d}} &= 4q_{\mathrm{AB}}\tau_c, \\
1/T_{2\mathrm{A}}^{(1)\mathrm{d}} &= 1/T_{2\mathrm{B}}^{(1)\mathrm{d}} = 8.5q_{\mathrm{AB}}\tau_c, \\
1/T_2^{(2)\mathrm{d}} &= 9q_{\mathrm{AB}}\tau_c, \\
W_0^{\mathrm{d}} &= q_{\mathrm{AB}}\tau_c, \qquad W_{1\mathrm{A}}^{\mathrm{d}} = W_{1\mathrm{B}}^{\mathrm{d}} = (3/2)q_{\mathrm{AB}}\tau_c, \qquad W_2 = 6q_{\mathrm{AB}}\tau_c.
\end{aligned}
\qquad [21]
$$

On the other hand, for long correlation times, $\tau_c \gg 1/\Omega$, in the *spin-diffusion limit*, we obtain

$$
\begin{aligned}
1/T_2^{(0)\mathrm{d}} &= q_{\mathrm{AB}}\tau_{\mathrm{c}}, \\
1/T_{2\mathrm{A}}^{(1)\mathrm{d}} &= 1/T_{2\mathrm{B}}^{(1)\mathrm{d}} = 2.5q_{\mathrm{AB}}\tau_{\mathrm{c}}, \\
1/T_2^{(2)\mathrm{d}} &= 0, \\
W_0^{\mathrm{d}} &= q_{\mathrm{AB}}\tau_{\mathrm{c}}, \qquad W_{1\mathrm{A}}^{\mathrm{d}} = W_{1\mathrm{B}}^{\mathrm{d}} = W_2^{\mathrm{d}} = 0.
\end{aligned}
\tag{22}
$$

(2) Relaxation by External Random Fields

We assume two random fields $B_{\mathrm{A}}(t)$ and $B_{\mathrm{B}}(t)$ acting on the two weakly coupled nuclei A and B, respectively. The random fields may originate from dipolar couplings to additional nuclei within or outside of the molecule considered or from paramagnetic impurities in the sample. The two random fields may be partially correlated, with the correlation coefficient

$$
C = \overline{B_{\mathrm{A}}B_{\mathrm{B}}}/(\overline{B_{\mathrm{A}}^2}\,\overline{B_{\mathrm{B}}^2})^{1/2}. \tag{23}
$$

This leads to the relaxation rates

$$
\begin{aligned}
1/T_2^{(0)\mathrm{r}} &= \frac{\gamma^2}{6}\{[\overline{B_{\mathrm{A}}^2} + \overline{B_{\mathrm{B}}^2} - 2C(\overline{B_{\mathrm{A}}^2}\,\overline{B_{\mathrm{B}}^2})^{1/2}]J(0) + (\overline{B_{\mathrm{A}}^2} + \overline{B_{\mathrm{B}}^2})J(\Omega)\}, \\
1/T_{2x}^{(1)\mathrm{r}} &= \frac{\gamma^2}{6}[\overline{B_x^2}J(0) + (\overline{B_{\mathrm{A}}^2} + \overline{B_{\mathrm{B}}^2})J(\Omega)], \\
1/T_2^{(2)\mathrm{r}} &= \frac{\gamma^2}{6}\{[\overline{B_{\mathrm{A}}^2} + \overline{B_{\mathrm{B}}^2} + 2C(\overline{B_{\mathrm{A}}^2}\,\overline{B_{\mathrm{B}}^2})^{1/2}]J(0) + (\overline{B_{\mathrm{A}}^2} + \overline{B_{\mathrm{B}}^2})J(\Omega)\}, \\
W_0^{\mathrm{r}} &= W_2^{\mathrm{r}} = 0, \\
W_{1x}^{\mathrm{r}} &= \frac{\gamma^2}{6}J(\Omega)\overline{B_x^2}, \qquad x = \mathrm{A},\ \mathrm{B}.
\end{aligned}
\tag{24}
$$

Let us assume in the following that the two random fields have equal variances, $\overline{B_{\mathrm{A}}^2} = \overline{B_{\mathrm{B}}^2} = \overline{B^2}$. In the *extreme narrowing limit*, $\tau_{\mathrm{c}} \ll 1/\Omega$, we then obtain the simplified expressions

$$
\begin{aligned}
1/T_2^{(0)\mathrm{r}} &= (2/3)\gamma^2\overline{B^2}\tau_{\mathrm{c}}[2 - C], \\
1/T_2^{(1)\mathrm{r}} &= \gamma^2\overline{B^2}\tau_{\mathrm{c}}, \\
1/T_2^{(2)\mathrm{r}} &= (2/3)\gamma^2\overline{B^2}\tau_{\mathrm{c}}[2 + C], \\
W_0^{\mathrm{r}} &= W_2^{\mathrm{r}} = 0, \\
W_1^{\mathrm{r}} &= (1/3)\gamma^2\overline{B^2}\tau_{\mathrm{c}}.
\end{aligned}
\tag{25}
$$

In the *spin-diffusion limit*, $\tau_{\mathrm{c}} \gg 1/\Omega$, on the other hand, we find

$$
\begin{aligned}
1/T_2^{(0)\mathrm{r}} &= (2/3)\gamma^2\overline{B^2}\tau_{\mathrm{c}}[1 - C], \\
1/T_2^{(1)\mathrm{r}} &= (1/3)\gamma^2\overline{B^2}\tau_{\mathrm{c}}, \\
1/T_2^{(2)\mathrm{r}} &= (2/3)\gamma^2\overline{B^2}\tau_{\mathrm{c}}[1 + C], \\
W_0^{\mathrm{r}} &= W_1^{\mathrm{r}} = W_2^{\mathrm{r}} = 0.
\end{aligned}
\tag{26}
$$

(c) Cross-Peaks in a 2D Exchange Spectrum

After this excursion to describe relaxation during the mixing process, we return to the calculation of the coherent and incoherent exchange processes during the mixing time which are responsible for the various cross-peaks in a 2D exchange spectrum. Following Eq. [17] and Fig. 3, we treat separately cross-peaks caused by the exchange of z magnetization, by the zero-quantum coherence and by the double-quantum coherence. Transverse magnetization or single-quantum coherence can be eliminated easily by a compensation experiment proposed in Ref. (*3*) and further described in Section IV. We therefore do not consider the effects of transverse interference caused by single-quantum coherence.

(1) Cross-Peaks Resulting from the Diagonal Elements of the Density Operator, $\sigma^{(z)}$

The diagonal part of the density matrix $\sigma(t_1, 0)$, Eq. [13], can be written in the operator form

$$\sigma^{(z)}(t_1, 0) = \alpha^{(z)}(t_1, 0)I_{Az} + \beta^{(z)}(t_1, 0)I_{Bz} \qquad [27]$$

with

$$\begin{aligned} \alpha^{(z)}(t_1, 0) &= -(1/2)\,\mathrm{Re}\{\alpha_1(t_1) + \alpha_2(t_1)\}, \\ \beta^{(z)}(t_1, 0) &= -(1/2)\,\mathrm{Re}\{\beta_1(t_1) + \beta_2(t_1)\}, \end{aligned} \qquad [28]$$

and with the coherence functions $\alpha_1(t_1)$, etc., of Eq. [12].

First, let us disregard relaxation and chemical exchange. The diagonal elements do not, in this case, change during the mixing period. They are transformed by the third $(\pi/2)_y$ pulse into the following coherence functions which can be observed during the detection period:

$$\begin{aligned} \alpha_1^{(z)}(t_1, \tau_m, t_2) &= -(1/4)(\cos \Omega_{A1}t_1 + \cos \Omega_{A2}t_1) \exp(i\Omega_{A1}t_1), \\ \alpha_2^{(z)}(t_1, \tau_m, t_2) &= -(1/4)(\cos \Omega_{A1}t_1 + \cos \Omega_{A2}t_1) \exp(i\Omega_{A2}t_2), \\ \beta_1^{(z)}(t_1, \tau_m, t_2) &= -(1/4)(\cos \Omega_{B1}t_1 + \cos \Omega_{B2}t_1) \exp(i\Omega_{B1}t_2), \\ \beta_2^{(z)}(t_1, \tau_m, t_2) &= -(1/4)(\cos \Omega_{B1}t_1 + \cos \Omega_{B2}t_1) \exp(i\Omega_{B2}t_2). \end{aligned} \qquad [29]$$

We assume that the x component of the magnetization,

$$\langle F_x \rangle(t_1, \tau_m, t_2) = \mathrm{Tr}\,\{F_x \sigma(t_1, \tau_m, t_2)\}, \qquad [30]$$

is detected and we obtain

$$\begin{aligned} \langle F_x \rangle(t_1, \tau_m, t_2) = &-(1/4)(\cos \Omega_{A1}t_1 + \cos \Omega_{A2}t_1)(\cos \Omega_{A1}t_2 + \cos \Omega_{A2}t_2) \\ &- (1/4)(\cos \Omega_{B1}t_1 + \cos \Omega_{B2}t_1)(\cos \Omega_{B1}t_2 + \cos \Omega_{B2}t_2). \end{aligned} \qquad [31]$$

Equation [29] demonstrates that the two mixing pulses cause an equal distribution of the total A-spin (or B-spin) coherence $\cos \Omega_{A1}t_1 + \cos \Omega_{A2}t_1$ (or $\cos \Omega_{B1}t_1 + \cos \Omega_{B2}t_1$) among the transitions A_1 and A_2 (or B_1 and B_2). It leads to a coherence exchange among the components within each multiplet and to pairs of auto- and cross-peaks equal in phase and intensity within the diagonal A and B multiplets. This is shown in Fig. 4.

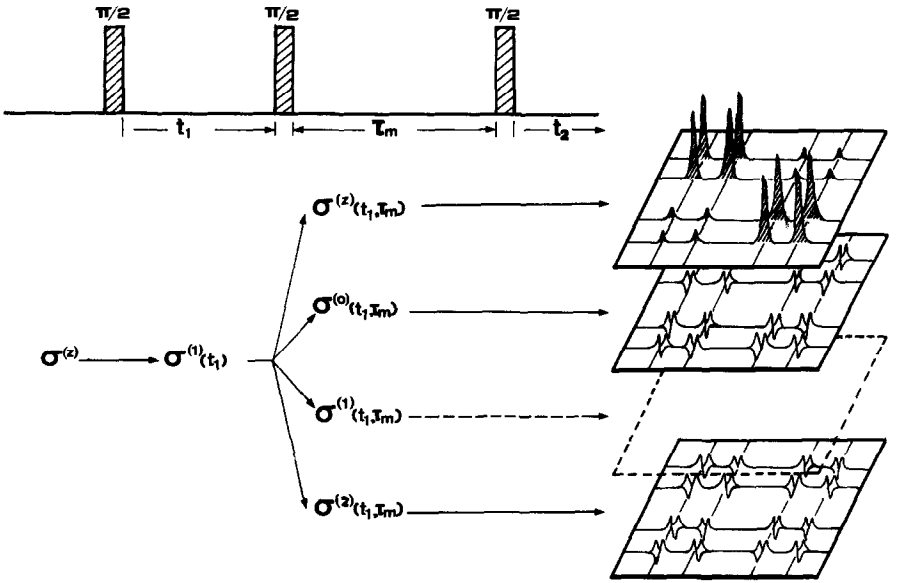

FIG. 4. Buildup of a 2D exchange spectrum from its constituent parts: $\sigma^{(z)}$ leads to exchange cross-peaks in the form of cross-peak multiplets equal in intensity in 2D absorption mode. $\sigma^{(0)}$ causes 2D dispersive auto- and cross-peaks all equal in absolute intensity but with alternating signs. The contribution from $\sigma^{(1)}$ is normally suppressed experimentally. $\sigma^{(2)}$ produces 2D dispersive auto- and cross-peaks equal in absolute intensity. The sign pattern is different for the zero-quantum and double-quantum contributions.

Let us now consider the additional effects of cross-relaxation or of chemical exchange during the mixing time. The density operator $\sigma^{(z)}(t_1, 0)$ of Eq. [27] is equivalent to the case of a two-spin system without spin–spin coupling. We can therefore directly use the results derived in Ref. (*3*) for an uncoupled spin system.

For the density operator at the end of the mixing period we find

$$\sigma^{(z)}(t_1, \tau_m) = \alpha^{(z)}(t_1, \tau_m) I_{Az} + \beta^{(z)}(t_1, \tau_m) I_{Bz} \qquad [32]$$

with

$$\begin{aligned} \alpha^{(z)}(t_1, \tau_m) &= \alpha^{(z)}(t_1, 0) \cdot a_{AA}(\tau_m) + \beta^{(z)}(t_1, 0) \cdot a_{BA}(\tau_m), \\ \beta^{(z)}(t_1, \tau_m) &= \alpha^{(z)}(t_1, 0) \cdot a_{AB}(\tau_m) + \beta^{(z)}(t_1, 0) \cdot a_{BB}(\tau_m). \end{aligned} \qquad [33]$$

The mixing coefficients $a_{AA}(\tau_m) \cdots$ are given by Eq. [25] of Ref. (*3*):

$$a_{AA}(\tau_m) = a_{BB}(\tau_m) = (1/2) \exp(-R_L \tau_m)[1 + \exp(-R_C \tau_m)]$$

and

$$a_{AB}(\tau_m) = a_{BA}(\tau_m) = \pm(1/2) \exp(-R_L \tau_m)[1 - \exp(-R_C \tau_m)], \qquad [34]$$

where the plus sign applies to chemical exchange and cross-relaxation near the spin-diffusion limit and the minus sign to cross-relaxation near extreme narrowing. When we assume equal efficiencies for the external random field relaxations for nuclei A and B, i.e., $W_{1A}^r = W_{1B}^r = W_1^r$, we find for the leakage relaxation rate R_L and for the cross-relaxation rate R_C

$$R_L = 2W_1^d + 2W_1^r + W_0^d + \frac{1}{\tau_{AB}} + W_2^d - \left| W_2^d - W_0^d - \frac{1}{\tau_{AB}} \right| ,$$

$$R_C = \left| W_2^d - W_0^d - \frac{1}{\tau_{AB}} \right| . \qquad [35]$$

The transition probabilities W are given by Eqs. [18], [21], [22], and [24]–[26].

It is essential to note that the A-spin and B-spin z-magnetization functions $\alpha^{(z)}(t_1, 0)$, $\beta^{(z)}(t_1, 0)$ which are involved in the exchange process, Eq. [33], contain the coherence functions $\alpha_1(t_1)$, $\alpha_2(t_1)$ and $\beta_1(t_1)$, $\beta_2(t_1)$, respectively. This means that the "entire multiplet" exchanges. We find therefore in the 2D spectrum cross-peak multiplets with four peaks equal in intensity whenever exchange takes place. This behavior is sketched in Fig. 4.

(2) J Cross-Peaks Due to Zero-Quantum Coherence

In the slow exchange limit, the zero-quantum coherence elements (23) and (32) of Eq. [13] precess during the mixing time τ_m with the difference frequency $\Omega_A - \Omega_B$ and are transformed by the third $(\pi/2)_y$ pulse into the following single-quantum coherence components (neglecting relaxation):

$$\alpha_1^{(0)}(t_1, \tau_m, t_2) = \frac{i}{8}(-\sin \Omega_{A1}t_1 + \sin \Omega_{A2}t_1 + \sin \Omega_{B1}t_1 - \sin \Omega_{B2}t_1) \times \cos [(\Omega_A - \Omega_B)\tau_m] \exp(i\Omega_{A1}t_2),$$

$$\alpha_2^{(0)}(t_1, \tau_m, t_2) = \frac{i}{8}(\sin \Omega_{A1}t_1 - \sin \Omega_{A2}t_1 - \sin \Omega_{B1}t_1 + \sin \Omega_{B2}t_1) \times \cos [(\Omega_A - \Omega_B)\tau_m] \exp(i\Omega_{A2}t_2), \qquad [36]$$

$$\beta_1^{(0)}(t_1, \tau_m, t_2) = \frac{i}{8}(\sin \Omega_{A1}t_1 - \sin \Omega_{A2}t_1 - \sin \Omega_{B1}t_1 + \sin \Omega_{B2}t_1) \times \cos [(\Omega_A - \Omega_B)\tau_m] \exp(i\Omega_{B1}t_2),$$

$$\beta_2^{(0)}(t_1, \tau_m, t_2) = \frac{i}{8}(-\sin \Omega_{A1}t_1 + \sin \Omega_{A2}t_1 + \sin \Omega_{B1}t_1 - \sin \Omega_{B2}t_1) \times \cos [(\Omega_A - \Omega_B)\tau_m] \exp(i\Omega_{B2}t_2).$$

The phase of these terms is in quadrature to those of Eq. [29] and the resulting peaks will be dispersive when the contributions of Eq. [29] are phase adjusted to become absorptive. The zero-quantum coherence terms contribute in equal amount (except for the signs) to all possible auto- and cross-peaks of the 2D spectrum including the cross-peaks within and between the A and B multiplets (cf. Fig. 4). Their intensities are cosine modulated by the zero-quantum precession during the mixing time τ_m with the precession frequency $\Omega_A - \Omega_B$. Because of this dependence on $\cos (\Omega_A - \Omega_B)\tau_m$, intensities and signs of the J cross-peaks may vary within one spectrum of a multispin system from multiplet to multiplet.

The maximum intensities are obtained for vanishingly short mixing time and are identical to those of the maximum NOE or chemical exchange cross-peaks.

Zero-quantum cross-peaks are attenuated by the zero-quantum relaxation during the mixing time and their intensities are proportional to $\exp(-\tau_m/T_2^{(0)})$. The zero-quantum coherence is relaxed, according to Eqs. [21] and [22], by dipolar relaxation in the extreme narrowing as well as in the spin-diffusion limit. In addition, there is normally also a contribution from random field relaxation. However, it should be noted that zero-quantum coherence is not affected by completely correlated random fields equal in strength nor by magnetic field inhomogeneity. Chemical exchange between A and B will lead to an additional attenuation proportional to $\exp(-\tau_m/\tau_{AB})$ (Eq. [16]).

(3) J Cross-Peaks Due to Double-Quantum Coherence

Double-quantum coherence existing during the mixing period causes the following transverse magnetization during the detection period (we again suppress relaxation terms for simplicity):

$$\begin{aligned}
\alpha_1^{(2)}(t_1, \tau_m, t_2) &= \frac{i}{8}\{-\sin \Omega_{A1}t_1 + \sin \Omega_{A2}t_1 - \sin \Omega_{B1}t_1 + \sin \Omega_{B2}t_1\} \\
&\quad \times \cos[(\Omega_A + \Omega_B - 2\omega_1)\tau_m] \exp(i\Omega_{A1}t_2), \\
\alpha_2^{(2)}(t_1, \tau_m, t_2) &= \frac{i}{8}\{\sin \Omega_{A1}t_1 - \sin \Omega_{A2}t_1 + \sin \Omega_{B1}t_1 - \sin \Omega_{B2}t_2\} \\
&\quad \times \cos[(\Omega_A + \Omega_B - 2\omega_1)\tau_m] \exp(i\Omega_{A2}t_2), \\
\beta_1^{(2)}(t_1, \tau_m, t_2) &= \frac{i}{8}\{-\sin \Omega_{A1}t_1 + \sin \Omega_{A2}t_1 - \sin \Omega_{B1}t_1 + \sin \Omega_{B2}t_1\} \\
&\quad \times \cos[(\Omega_A + \Omega_B - 2\omega_1)\tau_m] \exp(i\Omega_{B1}t_2), \\
\beta_2^{(2)}(t_1, \tau_m, t_2) &= \frac{i}{8}\{\sin \Omega_{A1}t_1 - \sin \Omega_{A2}t_2 + \sin \Omega_{B1}t_1 - \sin \Omega_{B2}t_1\} \\
&\quad \times \cos[(\Omega_A + \Omega_B - 2\omega_1)\tau_m] \exp(i\Omega_{B2}t_2).
\end{aligned} \tag{37}$$

It is interesting to note that for short mixing time, $\tau_m \to 0$, the AB cross-terms due to the double-quantum coherence exactly cancel the corresponding zero-quantum cross-terms of Eq. [36]. On the other hand, the zero- and double-quantum effects on the autopeaks and on the AA and BB cross-peaks are additive (cf. Fig. 4). The dependence of the amplitude of the double-quantum J cross-peaks on the mixing time τ_m is determined here by the sum of the two Larmor frequencies $\Omega_A + \Omega_B - 2\omega_1$. It is often a rapidly varying function of τ_m.

Double-quantum coherence is quite efficiently relaxed by dipolar relaxation in the extreme narrowing limit, Eq. [21]. However, in the spin-diffusion limit, the dipolar AB interaction no longer affects the double-quantum coherence (cf. Eq. [22]) and, consequently, the double-quantum J cross-peaks may become considerably stronger than the zero-quantum J cross-peaks in this limit. External

random field relaxation attenuates the double-quantum J cross-peaks, even for completely correlated random fields (Eq. [24]). In addition, double-quantum coherence is quite sensitive to magnetic field inhomogeneity (*22*). However, it is not affected by chemical exchange (cf. Eq. [16]).

(d) Numerical Examples of Cross-Peak Intensities

In this section we discuss three characteristic cases of cross-relaxation in the weakly coupled two-spin system. We assume the use of the dual phase-shifted experiment of Eq. [41] which suppresses J cross-peaks due to single-quantum coherence but leaves zero-quantum and double-quantum J cross-peaks unaffected.

(1) Cross-Relaxation near Extreme Narrowing Conditions

We assume a two-spin-1/2 system with exclusively intramolecular AB dipolar relaxation in a low-viscosity solution with $\Omega\tau_c = 0.0628$, $\Omega/2\pi = 100$ MHz, and $\tau_c = 10^{-10}$ sec. Figure 5 shows the auto- and cross-peak intensities plotted as functions of the mixing time τ_m. The intensities are normalized to the maximum autopeak intensity (reached for $\tau_m = 0$) and refer to signals phase adjusted to 2D absorption mode. The peak values of the corresponding 2D dispersion-mode signals are smaller by a factor of 4.

In Figs. 5A and B, a homogeneous magnetic field has been assumed. The NOE contribution to the autopeak intensities decays biexponentially for increasing mixing time τ_m while the cross-peaks increase to a maximum (negative) intensity of approximately 0.19 and then also decay to zero. The dispersive J-peak contributions (cf. Fig. 4), originating from zero- and double-quantum coherence, decay exponentially with the time constants $1/T_2^{(0)} = 4.00 q_{AB}\tau_c$ and $1/T_2^{(2)} = 8.90 \times q_{AB}\tau_c$. For Fig. 5, we assume $q_{AB}\tau_c = 0.06$ sec^{-1}. For a longer mixing time, the zero-quantum contribution with the characteristic slow precession frequency dominates. For the autopeaks, the NOE and J-peak contributions are equal in amplitude for $\tau_m = 0$ and remain comparable in amplitude for $\tau_m \neq 0$. The cross-peaks, on the other hand, are dominated by the J-peak contribution which may become larger than the maximum NOE cross-peak intensity by as much as a factor of 5. At $\tau_m = 0$, zero- and double-quantum contributions to the cross-peaks compensate each other exactly and the J cross-peak intensity starts at zero for $\tau_m = 0$.

Figures 5C and D show peak intensities in the presence of an inhomogeneous static magnetic field. The double-quantum contribution is affected exclusively. It decays fast for increasing mixing time (*22*).

An experimental example of J cross-peak intensities is presented in Fig. 6. The intensity of a cross-peak in the 2D proton spectrum of 1,2-dibromothiophene is plotted as a function of τ_m for two ranges of τ_m values, (A) 0.19 sec $\leq \tau_m \leq$ 0.23 sec and (b) 1.50 sec $\leq \tau_m \leq$ 1.56 sec. The indicated points stem from experimental measurements of the peak intensities in phase-sensitive 2D spectra. The solid line originates from a computer simulation with the following parameters: $\Omega_A/2\pi - \omega_1 = 171.8$ Hz, $\Omega_B/2\pi - \omega_1 = 140.5$ Hz, $T_2^{(0)} = 0.31$ sec, $T_2^{(2)} = 0.69$ sec. In addition, a Gaussian broadening of the double-quantum transition by magnetic field inhomogeneity had to be assumed, causing a further damping of the double-

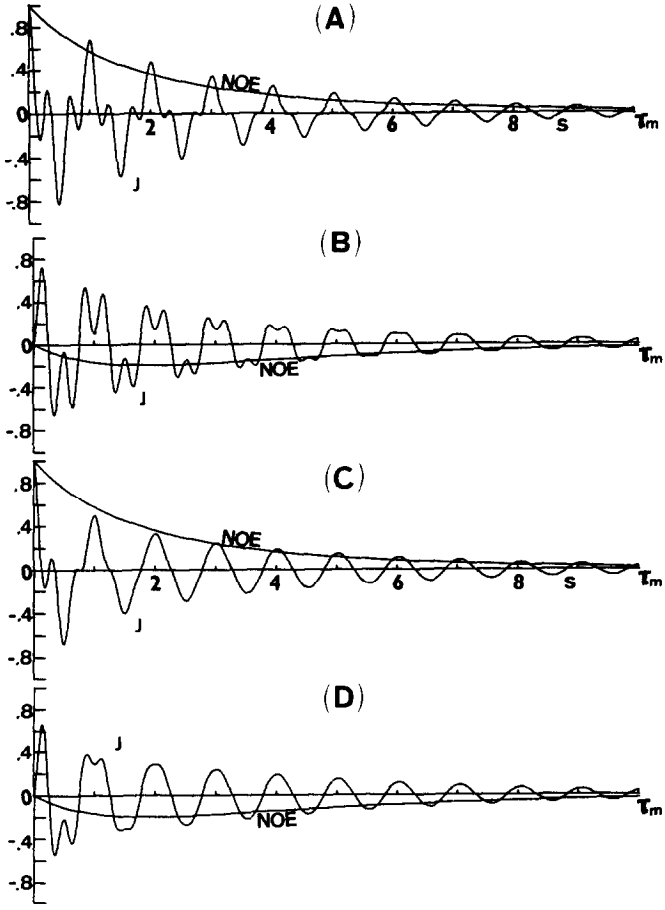

FIG. 5. Auto- and cross-peak intensities in a 2D NOE spectrum of a weakly coupled two-spin system near the extreme narrowing approximation for $\Omega\tau_c = 0.0628$, $\Omega/2\pi = 100$ MHz, and $\tau_c = 10^{-10}$ sec. The 2D absorptive NOE peaks and 2D dispersive contributions of J peaks are shown separately as functions of the mixing time τ_m. z magnetization and zero-quantum and double-quantum coherence have been considered. Single-quantum coherence is assumed to be eliminated. (A) Autopeak intensities in homogenous static field. (B) Cross-peak intensities in homogenous static field. (C) Autopeak intensities in inhomogenous static field causing an additional damping of the double-quantum coherence proportional to $\exp(-1.4\tau_m)$. (D) Cross-peak intensities under the same conditions as those in (C).

quantum coherence proportional to $\exp(-2\tau_m^2)$. At short mixing times, Fig. 6A, zero-quantum and double-quantum contributions are apparent while at longer mixing times, Fig. 6B, only the zero-quantum contribution remains appreciable in amplitude, because of rapid relaxation and defocusing of the double-quantum coherence. Cross-relaxation is negligible in this case.

(2) Cross-Relaxation for Intermediate Correlation Times

We consider here the case of an intermediate-sized molecule with a slow tumbling rate such that the correlation time τ_c fulfills the condition $\Omega\tau_c = 0.68$,

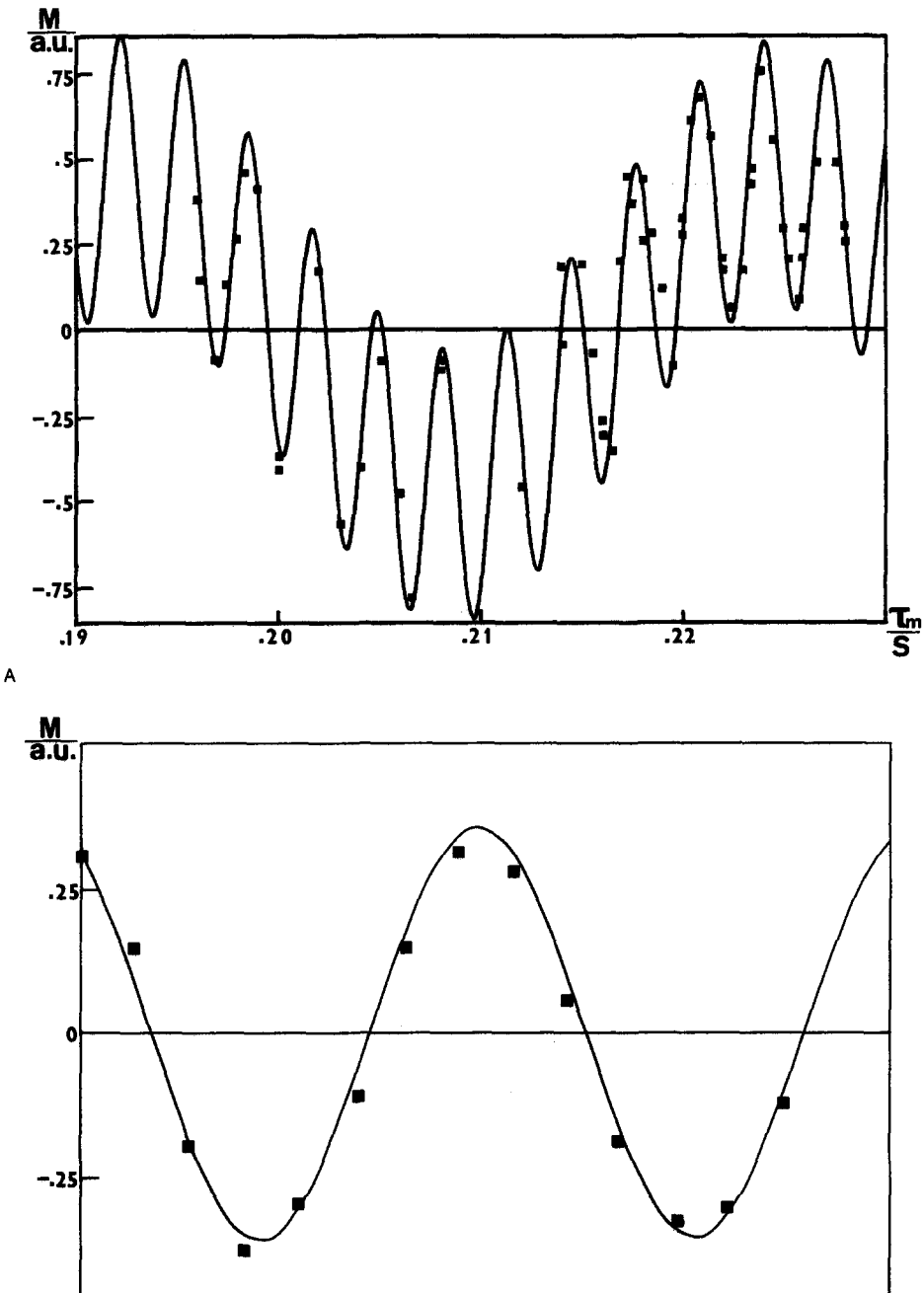

FIG. 6. Experimental cross-peak intensities for the two-spin proton system 1,2-dibromothiophene recorded at 90 MHz. Single-quantum coherence has been eliminated by a compensating phase-shifted dual experiment (cf. Section IV). The solid lines stem from a computer simulation with parameter values indicated in the text. Two restricted ranges of τ_m values are shown in (A) and (B).

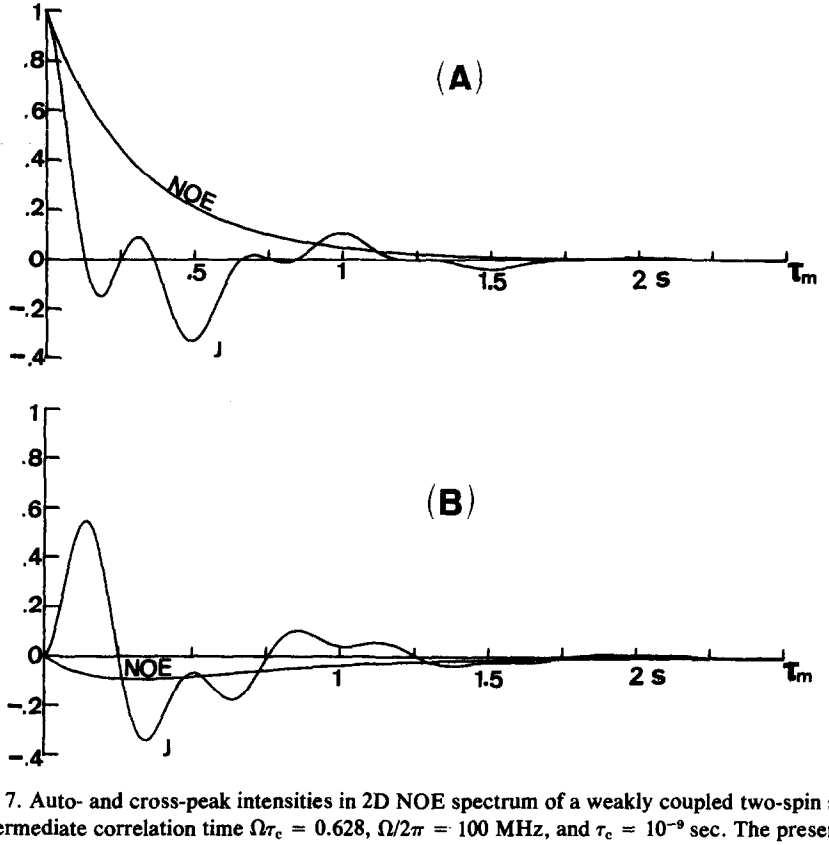

FIG. 7. Auto- and cross-peak intensities in 2D NOE spectrum of a weakly coupled two-spin system for intermediate correlation time $\Omega\tau_c = 0.628$, $\Omega/2\pi = 100$ MHz, and $\tau_c = 10^{-9}$ sec. The presentation is similar to that of Fig. 5. A homogeneous static magnetic field is assumed. (A) Autopeak intensities. (B) Cross-peak intensities.

$\Omega/2\pi = 100$ MHz, and $\tau_c = 10^{-9}$ sec. We assume exclusively dipolar relaxation caused by the AB interaction and obtain the following parameter values: $1/T_2^{(0)} = 3.15q_{AB}\tau_c$, $1/T_2^{(2)} = 4.48q_{AB}\tau_c$, $R_C = 2.65q_{AB}\tau_c$, $R_L = 4.15q_{AB}\tau_c$. The leakage relaxation rate is dominant. It strongly attenuates the NOE cross-peaks such that the J cross-peak contributions will primarily determine the cross-peak intensities unless J cross-peaks are purposely suppressed by the techniques described in Section IV.

Figure 7 gives the auto- and cross-peak intensities as functions of the mixing time τ_m assuming $q_{AB}\tau_c = 0.6$ sec^{-1}. The NOE cross-peaks are negative and reach a maximum value of approximately 0.09. For still slower tumbling, the NOE cross-peak intensities pass through zero and become positive when the spin-diffusion limit is approached.

(3) Cross-Relaxation near the Spin-Diffusion Limit

We assume a solution of large molecules with long rotational correlation time, $\Omega\tau_c = 6.28$, $\Omega/2\pi = 100$ MHz, and $\tau_c = 10^{-8}$ sec. In the spin-diffusion limit, $\Omega\tau_c \gg 1$, the leakage rate R_L and the double-quantum dipolar relaxation rate

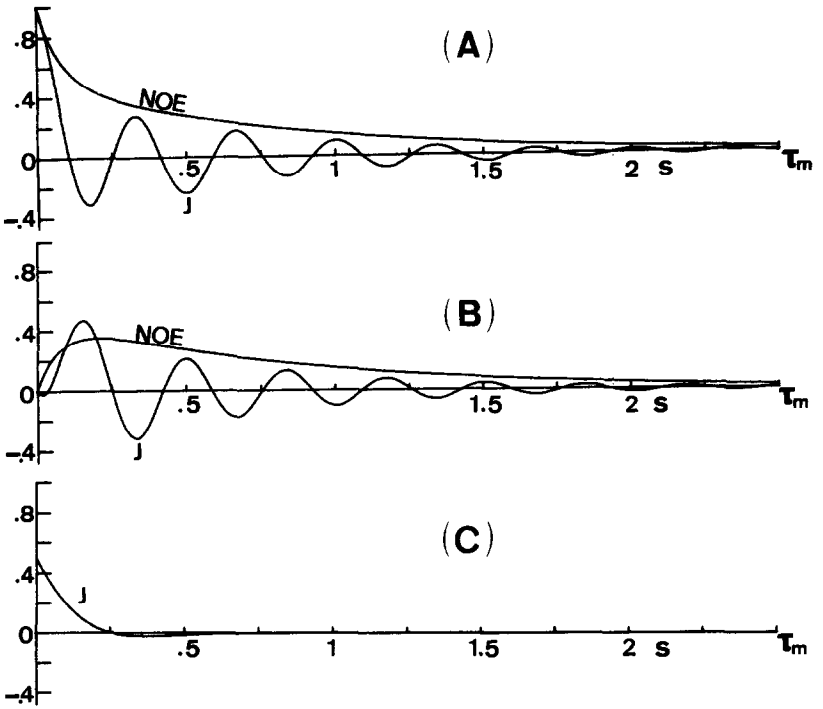

FIG. 8. Auto- and cross-peak intensities in 2D NOE spectrum of a weakly coupled two-spin system near the spin-diffusion limit for $\Omega\tau_c = 6.28$, $\Omega/2\pi = 100$ MHz, and $\tau_c = 10^{-8}$ sec. In addition to relaxation by dipolar AB interaction, uncorrelated random field relaxation with equal effects on both spins is assumed. The presentation is similar to that of Fig. 5. (A) Autopeak intensities. (B) Cross-peak intensities including zero-quantum and double-quantum J cross-peak contributions. (C) Separate plot of cross-peak contribution coming exclusively from zero-quantum coherence during the mixing period.

$1/T_2^{(2)}$ become zero. For a realistic model, it is therefore necessary to include interactions with further spins. We represent them by two uncorrelated external random fields equal in strength acting on spins A and B. We find the following rate constants:

$$\begin{aligned} 1/T_2^{(0)} &= 1.07 q_{AB}\tau_c + 1.01\gamma^2\overline{B^2}\tau_c', \\ 1/T_2^{(2)} &= 0.11 q_{AB}\tau_c + 1.01\gamma^2\overline{B^2}\tau_c', \\ R_C &= 1.93 q_{AB}\tau_c, \\ R_L &= 0.15 q_{AB}\tau_c + 0.35\gamma^2\overline{B^2}\tau_c'. \end{aligned} \qquad [38]$$

For the computer simulation, we used the values $q_{AB}\tau_c = 6$ sec^{-1} and $\gamma^2\overline{B^2}\tau_c' = 0.9$ sec^{-1}.

The resulting auto- and cross-peak intensities are presented in Fig. 8. The NOE autopeak intensity decays initially rapidly with the cross-relaxation rate R_C and reaches a state which slowly decays to zero with the much smaller leakage rate R_L. Here the NOE cross-peaks are positive and sizable in amplitude, approaching the maximum J cross-peak contributions arising from zero- or from double-

quantum coherence. The zero-quantum coherence decays rapidly to zero in a time of the order of $1/R_C$ while the double-quantum coherence persists for a much longer time and is damped primarily by external random field relaxation.

In the majority of practical applications of 2D exchange spectroscopy, 2D absolute-value spectra will be recorded. It is then no longer possible to distinguish exchange peaks and J peaks on the basis of their absorptive or dispersive character. In addition, cross-terms between the exchange and J-peak contributions will make the interpretation of the 2D spectra even more difficult.

The examples presented in this section make clear that it is necessary to design techniques for the complete suppression of the undesired J peaks. The following section is devoted to a discussion of such techniques.

IV. TECHNIQUES FOR ELIMINATING J CROSS-PEAKS

For the elimination of J cross-peaks due to the presence of single-quantum or double-quantum coherence during the mixing time, there are two simple and efficient techniques. However, the suppression of J cross-peaks due to zero-quantum coherence is more difficult. Let us consider first the suppression of single- and double-quantum coherence.

(a) Application of a Magnetic Field Gradient Pulse

A magnetic field gradient pulse applied in the course of the mixing period defocuses single-, double-, and higher-order coherence and leads to a rapid destruction of all elements of $\sigma^{(n)}$, $n \geq 1$. However, it does not affect longitudinal magnetization, $\sigma^{(z)}$, nor does it influence the zero-quantum coherence $\sigma^{(0)}$. The application of a magnetic field gradient pulse, although an efficient and simple means for suppressing part of the J cross-peak intensity, is undesirable in many circumstances as it interferes with the NMR field frequency lock system. It is often more convenient to apply phase-shifted pulse sequences as follows.

(b) Phase-Shifted Pulse Sequences

By the coaddition of the responses to phase-shifted pulse sequences it is possible to eliminate systematically the response of off-diagonal elements. This possibility relies on the fact that a simultaneous phase shift φ of the first two rf pulses causes a characteristic phase shift φ_m of the coherence components of $\sigma(t_1, 0)$ (*22*),

$$\varphi_m = m \cdot \varphi, \qquad m = 0, 1, 2, \ldots, \qquad [39]$$

for m-quantum coherence.

A dual experiment with the following pulse phases for the three pulses,

$$\begin{matrix} y & y & y \\ -y & -y & y, \end{matrix} \qquad [40]$$

and coaddition of the resulting responses leads, therefore, to the elimination of coherence $\sigma^{(m)}$ with $m = 1, 3, 5, \ldots$. An equivalent dual experiment

$$\begin{matrix} y & y & y \\ -y & y & -y \end{matrix} \qquad [41]$$

has the additional advantage of eliminating also at the same time the axial peaks which originate from transverse magnetization created exclusively by the last pulse (*3*). A quadruple experiment with the phases

$$\begin{matrix} y & y & y \\ -y & y & -y \\ x & x & y \\ -x & x & -y, \end{matrix} \qquad [42]$$

on the other hand, eliminates all coherence components up to $m = 3$ as well as the axial peaks.

When quadrature phase detection is employed for the distinction of positive and negative frequencies in ω_2, it is convenient to utilize in addition systematic phase cycling (*23*) leading to a total of 16 experiments. For quadrature phase detection in ω_1, finally, it is necessary to perform an additional set of experiments with the phases of the third pulse shifted by $\pi/2$. This then requires 32 independent experiments.

(c) Suppression of Zero-Quantum J Cross-Peaks

The sequences of the previous section do not affect the zero-quantum coherence which is insensitive to phase shifts, according to Eq. [39], as well as to magnetic field inhomogeneity.

As shown in Section III, *J* cross-peaks invariably form cross-peak multiplets with vanishing net intensity. In addition, they appear in quadrature phase with respect to the exchange and cross-relaxation cross-peaks which all have the same phase and sign. In a phase-sensitive spectrum, they can therefore be discovered easily. Two-dimensional *J* cross-peaks can also be identified by comparison with a conventional 2D autocorrelated spectrum obtained with a single $\pi/2$ mixing pulse (*5*). In such a spectrum "*J* cross-peaks" appear exclusively. However, one must take into consideration that cross-peaks may simultaneously receive contributions from coherent and incoherent transfer processes. In this case refined techniques are required to separate the two mechanisms.

In the following we describe three techniques which allow the suppression of zero-quantum *J* cross-peaks.

(1) Digital Filtering of the 2D Spectrum

By filtering of a 2D spectrum with a one-dimensional or two-dimensional filtering function with a width larger than the relevant *J* coupling constants, it is possible to suppress the *J* cross-peaks selectively because of the vanishing net intensity of *J* cross-peak multiplets. Such a filtering effect can be obtained either by restriction of the maximum t_1 or t_2 value in the sampling process or by a digital apodization in one or both of the two time domains. One may also consider convolution in the frequency domain.

(2) Random Variation of the Mixing Time τ_m

It has been demonstrated (Figs. 5–8) that the *J* cross-peak intensities depend in an oscillatory manner on the mixing time τ_m due to the coherent precession of

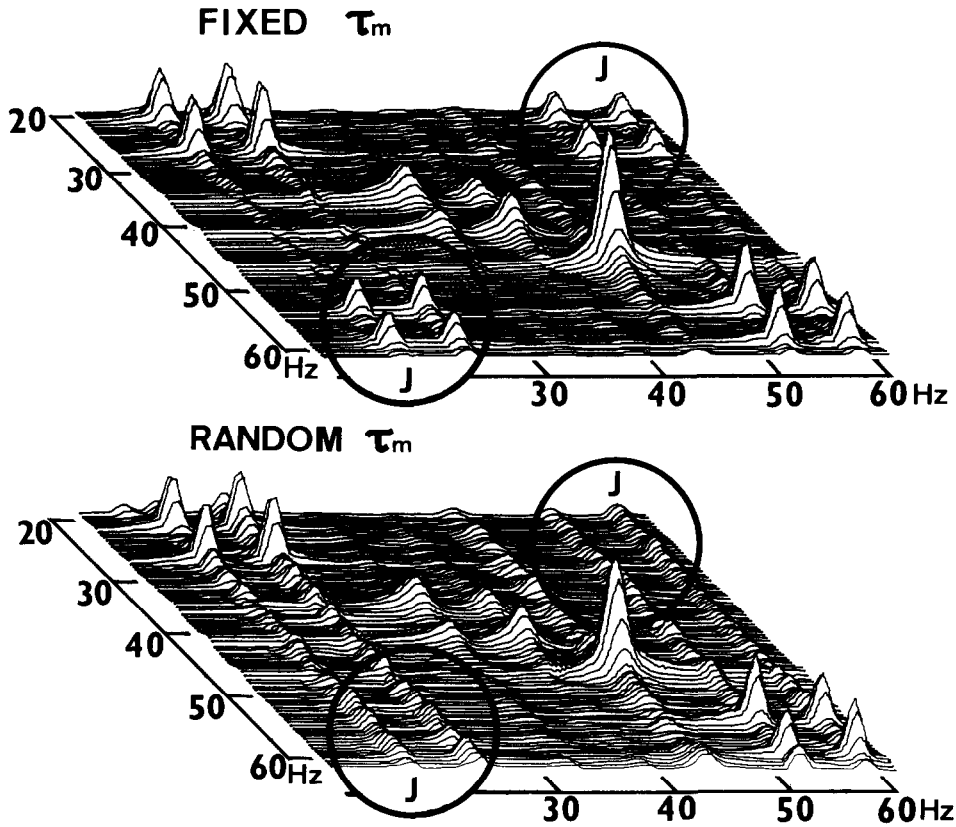

FIG. 9. Two-dimensional exchange spectra of a mixture of dimethylacetamide and 1,2-dibromothiophene. One hundred twenty-eight FIDs with t_1 values from 0 to 1024 msec have been recorded and submitted to a 2D Fourier transformation. A dual experiment according to Eq. [41] has been used to suppress single-quantum coherence and to eliminate the axial peaks. Top: A fixed mixing time τ_m = 212 msec is used. Bottom: The mixing time τ_m is varied randomly in the range $200 \leq \tau_m \leq 224$ msec for the 128 experiments with different t_1 values. The J cross-peaks are circled. The spectra are frequency folded to bring all resonance peaks into a narrow frequency region.

the zero- and double-quantum coherence. By coaddition of numerous free-induction decays from experiments with slightly different τ_m values, it is therefore feasible to suppress the J cross-peaks without significantly affecting the NOE or chemical exchange peaks. The variation of τ_m should cover at least one period of the smallest difference of resonance frequencies of coupled peaks in the sample.

Instead of or in addition to performing several complete 2D experiments with different τ_m values it is also feasible to vary τ_m randomly within a single 2D experiment at the same time that t_1 is varied systematically. This time-saving procedure leads to a smearing of J peaks in the direction of the ω_1 axis, causing an additional noise band instead of dominant peaks.

An example of such a J cross-peak elimination is shown in Fig. 9 by means of a test sample consisting of a mixture of dimethylacetamide (DMA) and of 1,2-dibromothiophene (DBT). DMA gives rise to chemical exchange cross-peaks apparent in the center of the spectrum. They are caused by the internal rotation

about the N–C bond. DBT, on the other hand, is a weakly coupled two-spin system and exhibits dominant J cross-peaks in the lower left and upper right corners of the 2D spectrum. Figure 9 gives two 2D spectra: with fixed τ_m value (top), and with random τ_m values (bottom). The selective disappearance of the J cross-peaks for random τ_m values is apparent. The slightly increased t_1 noise bands are due to the smearing effect mentioned. The exchange cross-peaks of DMA, on the other hand, are not affected by the randomization of τ_m.

(3) Partial Refocusing of the Zero-Quantum Evolution

A similar variation of the zero-quantum precession phase can be achieved by applying in the course of the mixing period of fixed length τ_m a 180° pulse at a random position which is varied from experiment to experiment. One finds that chemical exchange and cross-relaxation effects are not affected by the position of the 180° pulse. However, the zero-quantum evolution becomes partially refocused depending on the position of the additional pulse. This leads to a modulation of the amplitude and sign of the J cross-peaks which cancel upon addition of a sufficient number of experiments.

The three techniques described for the suppression of zero-quantum J cross-peaks also attenuate or randomize single- and multiple-quantum J cross-peaks. The use of the phase-shifted pulse sequences described in Section IVb, however, may still be desirable because they lead to exact cancellation of single- and double-quantum J cross-peaks.

For practical realizations of 2D exchange spectroscopy, it is thus recommended that the phase-shifted pulse sequences of Eq. [41] or Eq. [42] be used in combination with randomized τ_m values within each sequence of t_1 values. When quadrature phase detection is employed, the performance of additional experiments with systematic phase cycling is recommended.

The experiments shown in Figs. 6 and 9 were performed on a homemade 90-MHz spectrometer equipped with a Bruker 18-in. magnet and with a Varian 620/L-100 computer and a Diablo disk. A general 2D program slightly modified for the particular experiment was employed.

V. CONCLUSIONS

In most 2D cross-relaxation and chemical exchange studies coupled spin systems must be investigated. In such systems, coherent and incoherent exchange processes occur at the same time. It has been found that in many cases the coherent exchange processes leading to the J cross-peaks dominate. Although J cross-peaks contain valuable information on the coupled spin system, they must be suppressed for clarity of the spectrum. Several techniques suitable for this purpose have been described in this paper. The information contained in the J cross-peaks can be obtained more conveniently from a separate 2D-correlated spectrum (*5*, *9*).

For a complete 2D study of a system involving cross-relaxation or chemical exchange it is therefore necessary to record two 2D spectra, a 2D exchange spectrum with J effects eliminated for the elucidation of the exchange processes, and a 2D-correlated spectrum for the assignment of the coupling network. This pair of experiments forms a powerful tool, in particular for the study of biological macromolecules.

An instructive example demonstrating the importance of J cross-peaks in 2D NOE spectra of proteins for short mixing times will be published elsewhere (*24*).

ACKNOWLEDGMENTS

Partial support by the Swiss National Science Foundation and by a postdoctoral fellowship by the Research Fund of S. R. Serbia, Yugoslavia, to S.M. is acknowledged. The authors would like to thank Mr. M. Linder for extensive help and advice with regard to computer software. Some preliminary unpublished calculations of J coupling effects in 2D exchange spectroscopy have been performed by Dr. A. Wokaun. The authors are also indebted to Dr. Anil Kumar and Professor K. Wüthrich for several stimulating discussions. The manuscript was typed by Miss I. Müller.

REFERENCES

1. J. Jeener, B. H. Meier, P. Bachmann, and R. R. Ernst, *J. Chem. Phys.* **71,** 4546 (1979).
2. B. H. Meier and R. R. Ernst, *J. Am. Chem. Soc.* **101,** 6441 (1979).
3. S. Macura and R. R. Ernst, *Mol. Phys.* **41,** 95 (1980).
4. A. Kumar, R. R. Ernst, and K. Wüthrich, *Biochem. Biophys. Res. Commun.* **95,** 1 (1980).
5. W. P. Aue, E. Bartholdi, and R. R. Ernst, *J. Chem. Phys.* **64,** 2229 (1976).
6. A. Kumar, W. P. Aue, P. Bachmann, J. Karhan, L. Müller, and R. R. Ernst, *in* "Proceedings, XIXth Congress Ampere, Heidelberg, 1976," p. 473.
7. R. R. Ernst, W. P. Aue, P. Bachmann, J. Karhan, Anil Kumar and L. Müller, *in* "Proceedings, IVth Ampere International Summer School, Pula, Yugoslavia, 1976," p. 89.
8. K. Nagayama, K. Wüthrich, and R. R. Ernst, *Biochem. Biophys. Res. Commun.* **90,** 305 (1979).
9. K. Nagayama, A. Kumar, K. Wüthrich, and R. R. Ernst, *J. Magn. Reson.* **40,** 321 (1980).
10. H. M. McConnell, *J. Chem. Phys.* **28,** 430 (1958).
11. L. M. Jackman and F. A. Cotton, "Dynamic NMR Spectroscopy," Academic Press, New York, 1975.
12. J. I. Kaplan and G. Fraenkel, "NMR of Chemically Exchanging Systems," Academic Press, New York, 1980.
13. I. Solomon, *Phys. Rev.* **99,** 559 (1955).
14. A. Abragam, "Principles of Nuclear Magnetism," p. 333, Oxford Univ. Press, London, 1960.
15. J. S. Noggle and R. E. Schirmer, "The Nuclear Overhauser Effect. Chemical Applications," Academic Press, New York, 1971.
16. S. Alexander, *J. Chem. Phys.* **37,** 967, 974 (1962); **38,** 1787 (1963); **40,** 2741 (1964).
17. G. Binsch, *J. Am. Chem. Soc.* **91,** 1304 (1969).
18. J. I. Kaplan and G. Fraenkel, *J. Am. Chem. Soc.* **94,** 2907 (1972).
19. R. O. Kühne, T. Schaffhauser, A. Wokaun, and R. R. Ernst, *J. Magn. Reson.* **35,** 39 (1979).
20. A. G. Redfield, *IBM J. Res. Develop.* **1,** 19 (1957).
21. A. G. Redfield, *Advan. Magn. Reson.* **1,** 1 (1965).
22. A. Wokaun and R. R. Ernst, *Chem. Phys. Lett.* **52,** 407 (1977).
23. A. G. Redfield and S. D. Kunz, *J. Magn. Reson.* **19,** 250 (1975); E. O. Stejskal and J. Schaefer, *J. Magn. Reson.* **13,** 249 (1974), **14,** 160 (1974); D. J. Hoult and R. E. Richards, *Proc. Roy. Soc. Ser. A* **344,** 311 (1975).
24. A. Kumar, G. Wagner, R. R. Ernst, and K. Wüthrich, *J. Am. Chem. Soc.*, in press.